



Full-Scale Readout Electronics for the ECHo Experiment

Timo Muscheid¹ · Robert Gartmann¹ · Nick Karcher¹ · Felix Schuderer² ·
Martin Neidig² · Matthias Balzer¹ · Luis E. Ardila-Perez¹ · Sebastian Kempf^{2,1} ·
Oliver Sander¹

Received: 3 November 2023 / Accepted: 27 August 2024
© The Author(s) 2024

Abstract

Recent advances in the development of cryogenic particle detectors such as magnetic microcalorimeters allow the fabrication of sensor arrays with an increasing number of pixels. Since these detectors must be operated at the lowest temperatures, the readout of large detector arrays is still quite challenging. This is especially true for the ECHo experiment, which presently aims to simultaneously run 6,000 two pixel detectors to investigate the electron neutrino mass. For this reason, we developed a readout system based on a microwave SQUID multiplexer (μ MUX) that is operated by a custom software-defined radio (SDR) at room-temperature. The SDR readout electronics consist of three distinct hardware units: a data processing board with a Xilinx ZynqUS+ MPSoC; a converter board that features DACs, ADCs, and a coherent clock distribution network; and a radio frequency front-end board to translate the signals between the baseband and the microwave domains. Here, we describe the characteristics of the full-scale SDR system. First, the generated frequency comb for driving the μ MUX was evaluated. Subsequently, by operating the SDR in direct loopback, the crosstalk of the individual channels after frequency demultiplexing was investigated. Finally, the system was used with a 16-channel μ MUX to evaluate the linearity of the SDR, and the noise contributed to the overall readout setup.

Keywords Cryogenic detectors · Microwave SQUID multiplexer · Readout electronics · Software defined radio

✉ Timo Muscheid
timo.muscheid@kit.edu

¹ Institute for Data Processing and Electronics (IPE), Karlsruhe Institute of Technology (KIT), Karlsruhe, Germany

² Institute of Micro- and Nanoelectronic Systems (IMS), Karlsruhe Institute of Technology (KIT), Karlsruhe, Germany

1 Introduction

Experiments in various fields of physics, possibly containing hundreds of thousands of sensors, require state-of-the-art readout electronics capable of handling the ever-increasing data rates and performing real-time data analysis. Detectors working at cryogenic temperatures, such as the magnetic microcalorimeter (MMC), offer the highest energy resolutions, but simultaneously further complicate the readout architecture since the number of cables interfacing the cryogenic domain and the power dissipation at cryogenic temperatures need to be minimized. Specifically for MMCs, these challenges are tackled by Microwave-SQUID-Multiplexing (μ MUX) [1], which is a special kind of frequency multiplexing scheme that allows to readout many detectors on a single feedline. The ECHo experiment aims to investigate the mass of the electron neutrino by measuring the electron capture process of Holmium-163 [2] using the aforementioned MMCs. The released energy is measured by MMCs connected to a μ MUX [3], consisting of 400 resonators with resonance frequencies between 4 and 8 GHz and two MMC pixels each. In total, 800 detectors will be multiplexed on a single transmission line. In recent years, the readout concept, including the room-temperature electronics for online data analysis, has been demonstrated with various prototype iterations [4, 5]. Now, the system has been scaled up to target the total of 800 detectors per readout line. As the 12,000 sensors in the final experiment will be readout by 15 distinct units, the room-temperature software-defined radio (SDR) system presented and characterized in this work is the full-scale version of the system.

2 The Full-Scale SDR System

The concept of the custom room-temperature SDR readout is described in detail in previous publications [4, 6], including a schematic view. The room-temperature readout system follows a modular approach and consists of three distinct hardware units as seen in Fig. 1: a custom MPSoC board for digital signal processing [7], a conversion stage, and a heterodyne mixing stage [5].

The target frequency band between 4 and 8 GHz is divided into five subbands of 800 MHz each that operate independently from each other. The I and Q components of the frequency comb for resonator stimulation are generated digitally on



Fig. 1 Full-stack ECHo DAQ SDR electronics: digital processing board (left); analog/digital conversion board (center); high-frequency analog heterodyne mixer board (right)

the Programmable Logic (PL) and converted to the analog domain by DACs operated at 1 GHz. These baseband signals are subsequently shifted to individual band-pass signals by IQ mixers. When combined, they form a unified frequency comb, as seen in Fig. 2. On the receiving side, the modulated frequency comb is divided and downmixed similarly into five bands, sampled separately at 1 GHz by ADCs. The firmware running on the PL processes the five parallel data streams and performs channelization, flux-ramp demodulation, and event detection [8]. The resulting data streams containing the detector samples can be stored on the platform itself, or they can be sent to a client PC for post-processing and spectrum analysis.

3 System Characterization

Following final commissioning, the full-scale room-temperature readout electronics system was characterized. The measurement setups and results are presented in the following sections.

3.1 Frequency Comb Generation

The frequency comb generated by the SDR contains all the resonance frequencies needed to drive the multiplexer. The image rejection ratio (IRR) of the single tones is of main interest. Strong image frequencies increase the total power sent to the cryostat, potentially bring the HEMT amplifier into saturation, and are a severe source of crosstalk. These images are generated by phase and amplitude deviations of the I and Q components resulting from mismatches in the signal trace lengths from the DAC to the IQ mixer and component variation. By intentionally generating I and Q data with slightly different phases and amplitudes, these errors can be compensated. With all 400 tones enabled and operated off-resonance, the total signal power at the HEMT input is around -44 dBm in the worst case, which is slightly below the HEMT's input P1dB point of -42 dBm [9]. Calibrating the tones onto the resonators will additionally attenuate the signals; hence, the HEMT will be operated in the linear section. The TX-output of the SDR electronics was connected to a spectrum analyzer (Rohde & Schwarz FSWP50), and a frequency comb containing 80

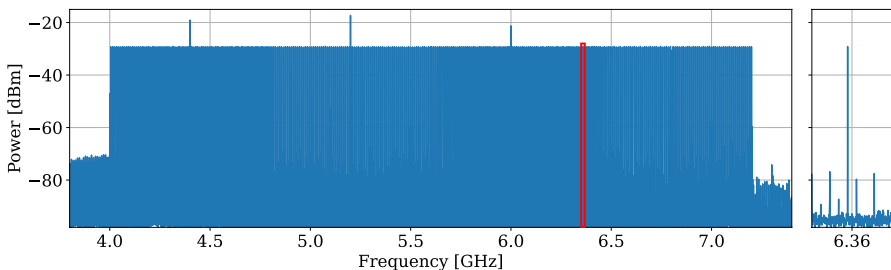


Fig. 2 Frequency comb containing 4 of 5 subbands with 80 tones each, where the IQ imbalance is corrected and the power is equalized for all tones. A selected tone is highlighted and zoomed in

random tones per subband was generated. After an IQ imbalance correction [10], the system reached an IRR > 40 dB; then limited by intermodulation and distortion in the following analog signal path. To obtain a flat comb, the weakest tone across the complete frequency band was detected, and the amplitude of all other tones was reduced to match that power. The signal power of individual tones can be adjusted by the users to match the requirements of the experiment. For ECHO in particular, the μ MUX, is designed for a signal power of -70 dBm per resonator [11]. The signal conditioning in the cryostat requires an input power of -27 dBm per tone at the cryogenic interface for optimal performance [12]. This requirement is being fulfilled by the presented system.

3.2 Channel Separation

As described in sect. 2, the wideband frequency comb is first divided into five subbands of 800 MHz each and mixed to the baseband. This analog band separation is evaluated by sweeping a single tone from 4 to 8 GHz and measuring the five baseband frequency responses of the standalone RF front-end. By applying an FFT, the strongest signal component for each input frequency was identified. The result of this measurement is shown on the left side of Fig. 3. The demodulator responsible for the frequency band between 6.4 and 7.2 GHz does not properly attenuate one of the clock signals, leading to a constant noise floor at around -67 dBm in this band. A minor revision of the RF front-end board will include the necessary modifications for optimization.

The ADCs provide internal digital down-conversion (DDC) and convert each analog baseband signal into two separate data streams with sampling rates of 500 MHz each, containing the upper and lower sidebands, respectively. The digital channelization is performed by a polyphase channelizer module that separates the 500 MHz signal into 32 equidistant channels with a passband of 11 MHz. Additionally, a second parallel polyphase channelizer module converts the frequency-shifted copy of the input signal into 32 channels that have their center frequency in the stopband of the first channelizer. In total, the digital channelization converts the 10 parallel 500 MHz bands into 64 overlapping channels each. Subsequently, a tunable numerically controlled oscillator (NCO) and a low-pass filter with a cutoff

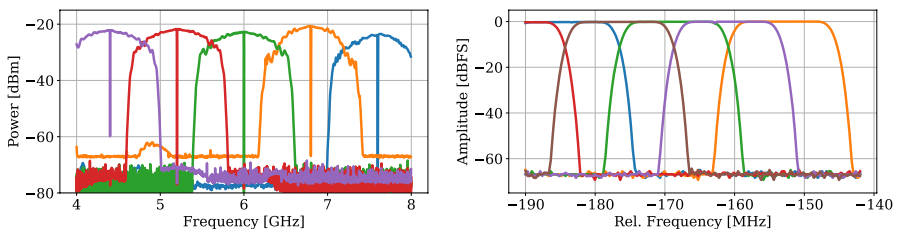


Fig. 3 Evaluation of the channel separation. First, the analog wideband comb is separated into 5 subbands with 800 MHz each (left). Then, a polyphase filter bank within the digital domain channelizes individual tones into a TDM scheme. For simplicity, only an extract of the digital filter bank for one data stream is shown (right)

frequency of 1.6 MHz are used on each channel to mix the carrier frequencies to DC. This specific cutoff frequency was chosen as a compromise between detector bandwidth and resource consumption, which increases with higher orders of the filter. The digital channel separation has been evaluated by generating a single tone in a room-temperature loopback configuration and measuring the output amplitudes of every channel. Across the full frequency band, digital crosstalk attenuation of more than 55 dB is achieved. An extract of the crosstalk after this channelization is shown on the right side of Fig. 3.

3.3 Noise Contribution

One critical aspect of the readout electronics is its contribution to the overall noise figure. For calculating the amplitude noise S_A of the readout electronics, the noise power spectral density (PSD) after digital down-conversion was compared in two scenarios: a direct room-temperature loopback and a full system with connection to the cryogenic domain, including a preliminary stack up of cryogenic and room-temperature amplifiers for boosting the signal power prior to the processing stage. The cryogenic setup for this measurement contained a μ MUX with 16 resonators located in the frequency range between 6.0 and 6.4 GHz. For a proper characterization of the final system with a 400 channel μ MUX and driving the HEMT at its intended point of operation, we emulated the remaining 384 tones across the full frequency range of 4–8 GHz. The amplitude of these additional tones was set to match the attenuated tones on the 16 resonators. From the perspective of the HEMT, this is equivalent to operating all 400 tones on the steepest gradient of the resonators. For the room-temperature loopback measurement, the tone power of all 400 tones was set to match the power at the RX-port of our electronics of the cryogenic measurement, in order to achieve a similar dynamic range of the ADCs.

The left side of Fig. 4 shows that the noise level of the room-temperature loopback is below the total noise of the cryogenic setup. Therefore, the room-temperature electronics are not the limiting factor for the measurement sensitivity.

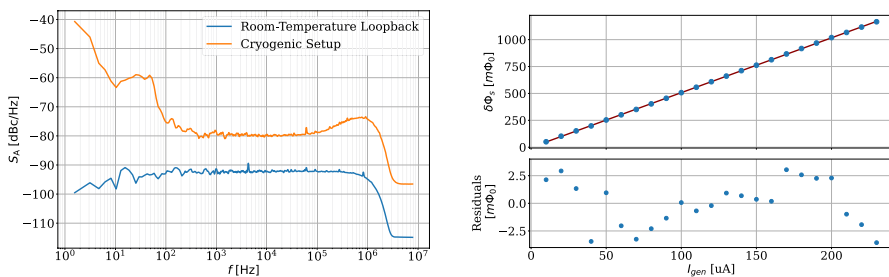


Fig. 4 Full SDR system characterization connected to the cryogenic domain. Left: Power spectral density (PSD) of the amplitude noise with 400 active tones, calculated from 10 million samples after down-conversion of the GHz carrier. The logarithmically spaced LPSD algorithm described in [14] was used for calculation. Right: Linearity on a single channel measured with a series of triangular input signals of increasing amplitude. The SDR response was calculated to $194 \pm 0.002 \mu\text{A}/\Phi_0$

3.4 System Linearity

For verification of the readout electronics under real conditions, it is required to include the μ MUX with sensing SQUIDs and phase modulating components in the signal path. To obtain a controlled measurement environment, we connected the input coil of each μ MUX SQUID to an external signal line via a superconducting flux transformer. This galvanic isolation was required since a direct connection strongly affected the μ MUX resonator quality. This MMC emulator setup allows us to inject known signals into individual μ MUX channels, e.g., to investigate the overall system linearity.

By using this MMC emulator, the system linearity of the SDR was evaluated. A linear response of the electronics is a key requirement to guarantee accurate measurements of the particle energy in the experiment. The linearity of the system is determined by taking consecutive measurements with increasing signal amplitude on the MMC emulator input. The input signal is then compared to the signal amplitude calculated by the SDR after channelization and flux-ramp demodulation. For this measurement, the Magnicom SQUID electronics [13] were connected to the MMC emulator as a signal source. The SQUID electronics were configured to generate sinusoidal and triangular signals with amplitudes up to $260\mu\text{A}$ to make sure that at least one magnetic flux quantum (Φ_0) is surpassed. The SDR response has a slope of $194 \pm 0.002\mu\text{A}/\Phi_0$ as shown in Fig. 4 on the right side. This measurement has been verified with a VNA (Keysight P5024B). Post-processing for reconstruction of the MMC emulator output resulted in a slope of $187\mu\text{A}/\Phi_0$. This deviation in the slope is not fully understood yet and needs further investigation.

4 Conclusion

While several prototypes of the SDR electronics had proved the readout concept successfully, the complete system with all components of signal generation and online data processing for 800 detectors has not been operated and evaluated yet. The system presented in this work allows the characterization of the interacting effects of up- and down-mixing of multiple parallel frequency bands together with analog and digital filtering for the first time ever. Analysis of the frequency comb testifies that the tones can be generated to match the multiplexer design, and the requirements of the cryogenic domain are fully met with an image rejection ratio and a signal-to-noise ratio above 40 dB. On the RX-side, the measurement results show excellent crosstalk attenuation at the analog and digital channel separation stages below 55 dB and an overall low noise contribution of the SDR. The measured linearity of the full system connected to the cryogenic domain at $194 \pm 0.002\mu\text{A}/\Phi_0$ promises accurate results once this system is utilized in the experiment. Overall, it was shown that readout of μ MUX signals is possible with high accuracy. The preliminary measurements with 400 tones promise low noise levels even for a large number of detectors.

Acknowledgements The authors acknowledge the support by the Doctoral School "Karlsruhe School of Elementary and Astroparticle Physics: Science and Technology"

Funding Open Access funding enabled and organized by Projekt DEAL.

Open Access This article is licensed under a Creative Commons Attribution 4.0 International License, which permits use, sharing, adaptation, distribution and reproduction in any medium or format, as long as you give appropriate credit to the original author(s) and the source, provide a link to the Creative Commons licence, and indicate if changes were made. The images or other third party material in this article are included in the article's Creative Commons licence, unless indicated otherwise in a credit line to the material. If material is not included in the article's Creative Commons licence and your intended use is not permitted by statutory regulation or exceeds the permitted use, you will need to obtain permission directly from the copyright holder. To view a copy of this licence, visit <http://creativecommons.org/licenses/by/4.0/>.

References

1. K.D. Irwin, J.A. Beall, W.B. Doriese, W.D. Duncan, G.C. Hilton, J.A.B. Mates, C.D. Reintsema, D.R. Schmidt, J.N. Ullom, L.R. Vale, B.L. Zink, K.W. Lehnert, Microwave squid multiplexers for low-temperature detectors. *Nuclear Instrum. Methods Phys. Res. Sect. A: Accel. Spectrom. Detect. Assoc. Equip* **559**(2), 802–804 (2006). <https://doi.org/10.1016/j.nima.2005.12.144>
2. L. Gastaldo, The electron capture in ^{163}Ho experiment - ECHO. *Eur. Phys. J. Spec. Topics* **226**(8), 1623–1694 (2017). <https://doi.org/10.1140/epjst/e2017-70071-y>
3. M. Wegner, N. Karcher, O. Krömer, D. Richter, F. Ahrens, O. Sander, S. Kempf, M. Weber, C. Enss, Microwave squid multiplexing of metallic magnetic calorimeters: status of multiplexer performance and room-temperature readout electronics development. *J. Low Temp. Phys.* **193**(3), 462–475 (2018). <https://doi.org/10.1007/s10909-018-1878-3>
4. O. Sander, N. Karcher, O. Krömer, S. Kempf, M. Wegner, C. Enss, M. Weber, Software-defined radio readout system for the ECHO experiment. *IEEE Trans. Nucl. Sci.* **66**(7), 1204–1209 (2019). <https://doi.org/10.1109/TNS.2019.2914665>
5. R. Gartmann, N. Karcher, R. Gebauer, O. Krömer, O. Sander, Progress of the ECHO SDR Readout Hardware for Multiplexed MMCs. *J. Low Temp. Phys.* (2022). <https://doi.org/10.1007/s10909-022-02854-1>
6. N. Karcher, D. Richter, F. Ahrens, R. Gartmann, M. Wegner, O. Krömer, S. Kempf, C. Enss, M. Weber, O. Sander, Sdr-based readout electronics for the echo experiment. *J. Low Temp. Phys.* **200**(5), 261–268 (2020). <https://doi.org/10.1007/s10909-020-02463-w>
7. T. Muscheid, A. Boebel, N. Karcher, T. Vanat, L. Ardila-Perez, I. Cheviakov, M. Schleicher, M. Zimmer, M. Balzer, O. Sander, Dts-100g - a versatile heterogeneous mpoc board for cryogenic sensor readout. *J. Instrum.* **18**(02), 02067 (2023). <https://doi.org/10.1088/1748-0221/18/02/C02067>
8. N. Karcher, T. Muscheid, T. Wolber, D. Richter, C. Enss, S. Kempf, O. Sander, Online demodulation and trigger for flux-ramp modulated SQUID signals. *J. Low Temp. Phys.* (2022). <https://doi.org/10.1007/s10909-022-02858-x>
9. LNF-LNC4_8F_LG. https://lownoiseactory.com/product/lmf-lnc4_8f_lg/. Accessed: 2024-07-24
10. E. Nash, Correcting imperfections in IQ modulators to improve RF signal fidelity (2009). <https://www.analog.com/media/en/technical-documentation/application-notes/AN-1039.pdf>
11. D.P. Richter, Multikanal-auslesung von metallischen magnetischen kalorimetern mittels eines vollständigen mikrowellen-squid-multiplexer-systems. In *PhD thesis*, Universität Heidelberg, Kichhoff Institut für Physik (2021). <https://doi.org/10.11588/heidok.00030266>
12. F.K. Ahrens, Cryogenic read-out system and resonator optimisation for the microwave squid multiplexer within the echo experiment. In *PhD thesis*, Universität Heidelberg, Kichhoff Institut für Physik (2022). <https://doi.org/10.11588/heidok.00032038>
13. D. Drung, C. Hinrichs, H.-J. Barthelmeß, Low-noise ultra-high-speed dc squid readout electronics. *Supercond. Sci. Technol.* **19**(5), 235 (2006). <https://doi.org/10.1088/0953-2048/19/5/S15>

14. M. Tröbs, G. Heinzel, Improved spectrum estimation from digitized time series on a logarithmic frequency axis. *Measurement* **39**(2), 120–129 (2006). <https://doi.org/10.1016/j.measurement.2005.10.010>

Publisher's Note Springer Nature remains neutral with regard to jurisdictional claims in published maps and institutional affiliations.